Environmental Science & Technology

Article

pubs.acs.org/est

Aggregation, Dissolution, and Transformation of Copper Nanoparticles in Natural Waters

Jon R. Conway,[†,§] Adeyemi S. Adeleye,[†,§] Jorge Gardea-Torresdey,[‡,§] and Arturo A. Keller*[,†,§]

[†]Bren School of Environmental Science and Management, University of California, Santa Barbara, California 93106, United States

[‡]Department of Chemistry, University of Texas at El Paso, El Paso, Texas 79968, United States

[§]University of California Center for the Environmental Implications of Nanotechnology (UC CEIN), Los Angeles, California, United States

Supporting Information

ABSTRACT: Time-dependent aggregation, sedimentation, dissolution, and transformation of three copper-based engineered nanomaterials (ENMs) of varied properties were measured in eight natural and artificial waters. Nano-Cu and $Cu(OH)_2$ aggregated rapidly to $>10^3$ nm while the aggregate size of nano-CuO averaged between 250 and 400 nm. Aggregate size for both nano-Cu and nano-CuO showed a positive correlation with ionic strength with a few exceptions. Aggregate size did not correlate well with sedimentation rate, suggesting sedimentation was influenced by other factors. Controlling factors in sedimentation rates varied by particle: $Cu(OH)_2$ particles remained stable in all waters but groundwater, nano-Cu was generally unstable except in waters with high organic content, and nano-CuO was stabilized by the presence of phosphate, which reversed surface charge polarity at concentrations as low as 0.1 mg PO_4^{3-} L^{-1}. Dissolution generally correlated with pH, although in saline waters, dissolved copper formed insoluble complexes. Nano-Cu was rapidly oxidized, resulting in dissolution immediately followed by the formation of precipitates. These results suggest factors including phosphate, carbonate, and ENM oxidation state may be key in determining Cu ENM behavior in natural waters.

1. INTRODUCTION

Although copper-based engineered nanomaterials (ENMs) currently comprise a relatively small fraction of global ENM production (~200 t per year as of 2010),[1] their toxicity and life cycle characteristics raise concerns regarding their environmental risk. For example, a common use for Cu-based ENMs is as the active ingredient in marine antifouling paints or agricultural biocides,[2] where they are directly introduced into the environment as intentionally toxic substances. Copper-based ENMs are somewhat unique among the most widely used ENMs in that they can participate in redox reactions to form three oxidation states: Cu^0, Cu^{1+}, and Cu^{2+}. Copper can also participate in a number of inorganic complexes with compounds found in natural waters, such as sulfate, sulfide, phosphate, chloride, and carbonate. The behavior of different Cu species in the environment is not well understood, and the formation of these various complexes may cause precipitation of ionic copper and alter the surface charge and therefore aggregation and dissolution kinetics of nanoparticulate copper. Solubility for the copper-based ENMs tested in this study have been seen to be enhanced at low pH and by the presence of organic coatings in previous research.[3] Additionally, several copper nanomaterials including Cu_2O and CuO have been shown to possess photocatalytic properties,[4−6] which may pose greater hazard to organisms if suspended in photic surface waters than if sedimented into aphotic sediments.

Size,[7] coating,[8] solubility,[9] and photoactivity[10,11] have all been implicated as playing roles in ENM toxicity and are all affected by water chemistry. Aggregate size (and consequently, sedimentation rate) is influenced by ionic strength (IS) and pH via charge regulation,[12,13] whereby the effective repulsive surface charge of the ENMs is decreased through ionic shielding and surface de/protonation. Depending on their composition, organic surface coatings can stabilize[14,15] or destabilize[8] particles in suspension and through the same mechanisms alter interactions between organisms and ENMs.[16,17] Previous research has shown that copper-based ENMs are toxic to a wide range of organisms, including fungi,[18] aquatic[19] and terrestrial plants,[20] estuarine amphipods,[21] daphnids and protozoa,[22] marine worms and clams,[23] and mussels.[24] It is therefore necessary to develop our understanding of how these materials behave once released into the environment in order to predict at-risk populations and properly regulate their manufacture, use, and disposal.

Received: October 8, 2014
Revised: January 14, 2015
Accepted: February 9, 2015
Published: February 9, 2015

DOI: 10.1021/es504918q
Environ. Sci. Technol. 2015, 49, 2749−2756

In this study, the physiochemical behaviors of three different species of Cu-based ENMs were quantified in eight natural and artificial waters covering a range of IS, pH, and organic content to gain insight into how these particles may behave in the environment. Additionally, equilibrium speciation modeling was performed to predict transformations of the Cu ENMs. Based on previous work, we hypothesized that aggregation would largely be controlled by the IS of the water, with more saline waters having greater aggregation due to surface charge shielding, and by the presence of dissolved organic matter that will increase electrostatic and steric repulsion between particles. Due to the propensity for larger, heavier aggregates to settle more rapidly, we hypothesized that sedimentation would be directly related to aggregation kinetics and hence controlled by IS and total organic content (TOC). We hypothesized that pH would be the key factor in dissolution with more dissolution occurring at lower pH and that the presence of TOC would also cause a small amount of dissolution. Additionally, we hypothesized that nano-Cu (as Cu^0) would have the greatest dissolution in oxic waters as it oxidized to Cu^{2+}.

2. METHODS

2.1. Characterization (Particles and Waters). Three particles were used in this study: nano-Cu (Sigma-Aldrich), nano-CuO (US Research Nanomaterials), and $Cu(OH)_2$ particles in the form of the commercial biocide Kocide 3000 (Dupont). A full characterization of the particles can be found in Adeleye et al.[3] and the Supporting Information for this paper (Figures S1−S7), and a summary is provided in Table 1.

Table 1. Physicochemical Properties of Particles Used in This Study (From Adeleye et al.[3])

property	Nano-CuO	Nano-Cu	$Cu(OH)_2$
primary particle diameter[a] (nm)	20−100	100−1000	100−1000
hydrodynamic diameter[b] (nm)	276 ± 12	1635 ± 501	1532 ± 580
copper content (wt %)	74.3 ± 1.2	83.3 ± 2.1	26.5 ± 0.9
other elements present[c]	C, O	C, O	C, O, Na, Al, Si, S, Zn
copper phase	monoclinic CuO	cubic Cu and Cu_2O	orthorhombic $Cu(OH)_2$
BET surface area (m^2/g)	12.31 ± 0.05	4.86 ± 0.03	15.71 ± 0.16
zeta potential[b] (mV)	−37.4 ± 0.7	−35.7 ± 1.3	−47.6 ± 4.3

[a]Dry powder measured with SEM. [b]Measured via DLS in Nanopure water at pH 7. [c]Analysis was done via XRD and EDS.

Briefly, the nano-Cu and nano-CuO ENMs were in the form of a high purity powder with primary particle sizes of 100−1000 and 20−100 nm, respectively. Kocide 3000 is composed of spherical composites on the order of 50 μm made up of irregular nano- to microscale $Cu(OH)_2$ particles embedded in a primarily carbon-based matrix that rapidly breaks down in water to release the $Cu(OH)_2$ particles. These can be seen in the inset of Figure S1. Kocide 3000 was chosen as a representative of commercially available nanocopper containing biocides, which often contain other ingredients like dispersants.

Properties of the five natural and three artificial waters used here can be found in Table 2, and details on collection and preparation can be found in the Supporting Information. Total organic carbon (TOC) content of the eight waters was determined using a Shimadzu TOC 5000 analyzer. Conductivity was measured with a traceable bench conductivity meter (Fisher Scientific), and pH was measured using a HACH HQ 40d portable meter. Elemental contents of water samples were quantified via ICP-AES (iCAP 6300, Thermo Scientific) except for Cl, which was measured with a chloride test kit (Hanna Instruments), and bicarbonate, which was measured with an alkalinity titration kit (LaMotte). Detection limits for TOC and PO_4^{3-} were 0.004 and 0.02 mg L^{-1}, respectively, and the detection limit for Al, Cu, and Fe was 0.05 mg L^{-1}. Ionic strength was calculated from the concentration of Ca^{2+}, Mg^{2+}, K^+, Na^+, HCO_3^-, SO_4^{2-}, and Cl^- using eq 1.

$$I = \frac{1}{2}\sum_{1=1}^{n} c_i Z_i^2 \quad (1)$$

where I is the ionic strength in mM, c_i is the concentration of the ith species in mM, and Z_i^2 is the oxidation number of the ith species.

2.2. Physicochemical Kinetics. Aggregation kinetics of Cu-based ENMs were measured by preparing 10 mg L^{-1} ENM suspensions in each water through dilution of a 100 mg L^{-1} stock, probe sonicating for 2 s at 20% amplitude (sufficient to disperse aggregates) with a Misonix Sonicator S-4000 (QSonica LLC, Newtown, CT), and then measuring size trends over time at 20 °C via dynamic light scattering (DLS, Zetasizer Nano ZS-90, Malvern Instruments). Measurements were taken every 30 s for 1 h. To measure sedimentation over time, the optical absorbency (Shimadzu 1601 UV−vis spectrophotometer) of suspensions identical to those described above were determined in triplicate every 6 min for 6 h at 320 nm with the exception of nano-Cu in lagoon water, seawater, and diluted seawater, which were measured at 520 nm at a concentration of 20 mg L^{-1}. Nano-Cu is the only of the three particles where copper is primarily in the zerovalent state, and as such it is able to participate in unique chemical reactions prior to oxidation to the +1 and +2 states. One of these is the temporary formation of copper(I) chloride compounds in saline waters (Figure S4), which absorbs strongly at 320 nm, the spectral wavelength that was used to detect solid copper. To test the effects of phosphate on nano-CuO, the sedimentation rates, ζ-potential (DLS, Zetasizer Nano ZS-90, Malvern Instruments), and pH of 10 mg L^{-1} nano-CuO in Nanopure water with the addition of 0, 0.1, 0.2, 0.5, 1, and 2 mg PO_4^{3-} L^{-1} (from NaH_2PO_4) were measured in triplicate.

To measure dissolution, ENM suspensions were prepared and stored at room temperature for 0, 1, 7, 14, 21, 30, 60, or 90 days, at which point they were transferred to Amicon Ultra-4 10 kDa centrifugal filter tubes (maximum pore size ∼3 nm, Millipore, Ireland) and centrifuged (Sorvall RC 5B Plus, CT) at 4000g for 40 min with a swinging bucket rotor. Filter retention was insignificant.[25] The filtrate was analyzed using a copper ion selective electrode (ISE, Cole Parmer, IL) under consistent lighting conditions to minimize light-induced interference. The filtrate was then oxidized with 1.2 vol % HNO_3 and 0.9 vol % H_2O_2 and analyzed for total copper content via inductively coupled plasma atomic emission spectroscopy (ICP-AES, iCAP 6300 Thermo Scientific, Waltham, MA), with a detection limit of 50 μg L^{-1}. Standard solutions were measured every 15 samples for quality assurance.

Two parameters related to dissolution were quantified: dissolved copper ($[Cu]_{dis}$), the total copper content of the ENMs present as free ions (Cu^{1+} and Cu^{2+}), and aqueous phase

DOI: 10.1021/es504918q
Environ. Sci. Technol. 2015, 49, 2749−2756

Table 2. Water Characteristics[a]

parameter	unit	Santa Barbara seawater	UCSB lagoon water	1/2 seawater dilution	wastewater	simulated groundwater	hydroponic media	storm runoff	simulated freshwater
pH		7.3	6.6	7.7	7.6	7.5	5.9	6.6	6.3
conductivity	μS	49400	50800	26100	2290	971	1317	271	119.7
IS	mM	770	676	381	34.1	12.1	11.2	4.4	0.8
TOC	mg C L^{-1}	ND	ND	ND	2.38	0	0	6.49	0.5
redox potential	mV	142	136	136	123	137	213	211	185
HCO_3	mg $CaCO_3$ L^{-1}	124	124	60	56	156	0	30	12
PO_4	mg L^{-1}	ND	0.23	ND	2.71	0	93	1.37	0.64
SO_4	mg L^{-1}	1900	2300	950	320	20	0	27.5	0
Cl	mg L^{-1}	20500	22500	10500	500	141	425	40	6.6
Na	mg L^{-1}	12700	12800	6350	325.37	158.08	0	49.3	0
Ca	mg L^{-1}	490	493	245	119.87	49.52	98.2	36.1	1.5
Mg	mg L^{-1}	1630	16.9	815	77.94	27.49	22.12	1	3.5
Al	mg L^{-1}	ND	ND	ND	ND	0	0	ND	0
K	mg L^{-1}	461	464	230	38.59	8.59	47.9	7.5	1.2
Cu	mg L^{-1}	ND	ND	ND	0.08	0	0.024	0.16	0.1
Fe	mg L^{-1}	ND	ND	ND	0.35	0	0.56	0.25	0.06

[a]ND = Not detected.

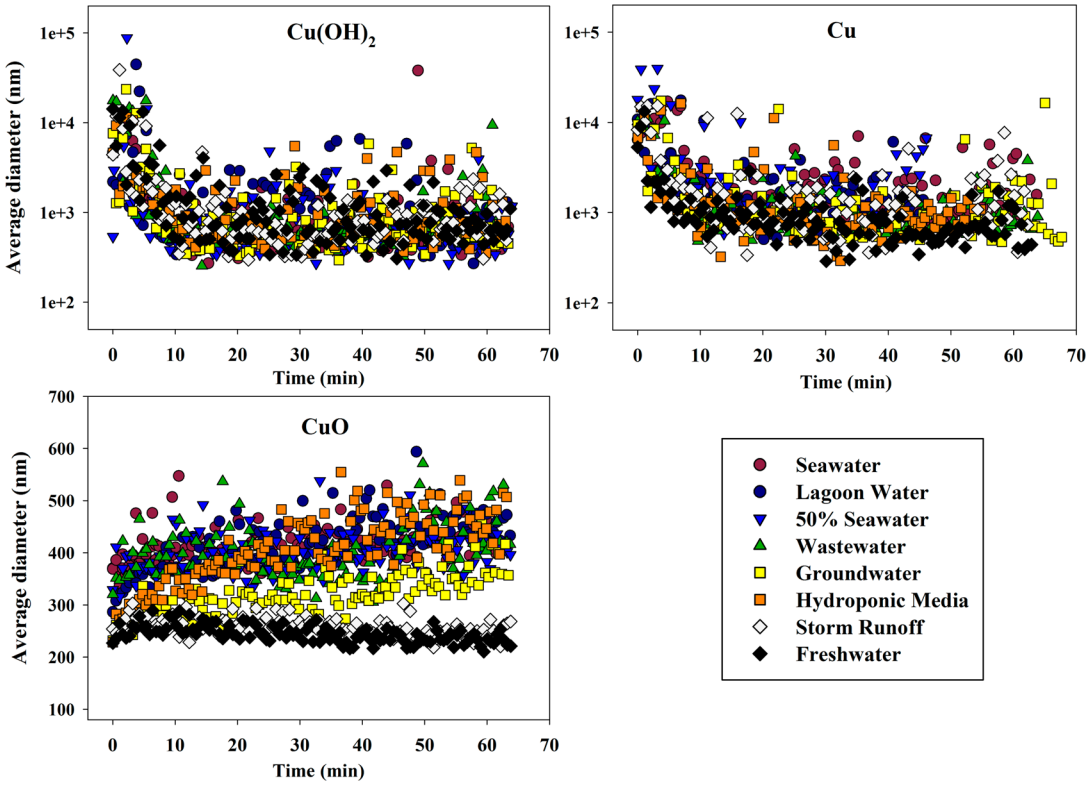

Figure 1. Aggregation kinetics for $Cu(OH)_2$, nano-Cu, and nano-CuO. Note variable scale of *y* axes.

copper ($[Cu]_{aq}$), the total copper content of the ENMs in the filtrate, which includes dissolved copper, complexed copper (e.g., CuCl, $CuCO_3$, $Cu_3(PO_4)_2$, etc.), and copper bound by ligands under 10 kDa. The ISE that was used to detect free ionic copper was capable of detecting both Cu^{1+} and Cu^{2+}, both of which may have been shed by the nano-Cu ENMs, but since Cu^{1+} undergoes rapid disproportionation[26] into Cu(0) and Cu^{2+} (E_{cell}^0 = +0.37 V) and is readily oxidized to Cu^{2+} in oxic water (E_{cell}^0 = +1.08 V), it is unlikely to be present as a free ion in any significant amount. Visual MINTEQ (v3.0) was used to predict speciation and complex formation in the natural waters based on the parameters given in Table 2. Additional information on model parameters can be found in the Supporting Information.

2.3. Statistical Analyses. To determine the effect of water type on aggregate size, one-way ANOVA or Kruskal–Wallis tests with posthoc Tukey's or multiple comparisons were performed. To verify the effect of time, linear models were fitted to each aggregation trend. All analyses were performed in Excel (Microsoft Office 2010) or RStudio (0.96.316).

DOI: 10.1021/es504918q
Environ. Sci. Technol. 2015, 49, 2749–2756

3. RESULTS AND DISCUSSION

3.1. Aggregation Kinetics. Aggregation of nano-Cu and $Cu(OH)_2$ particles (Figure 1) was characterized by three phases in the 1 h time period measured: (1) immediate aggregation to roughly 5−10 μm in the first few seconds postsonication, (2) a downward trend in aggregate size from 0 to 10 min that was likely due to sedimentation of the largest aggregates out of the water column, and (3) a stable phase in which aggregate diameters averaged 700−2000 nm. Aggregation of nano-Cu and nano-CuO followed the trends outlined in our hypothesis (i.e., enhanced aggregation at high IS and low TOC) with a few instructive exceptions discussed below, but $Cu(OH)_2$ had similar aggregation behaviors in all waters.

The polydispersity indices (PDIs) reported from the DLS analysis for $Cu(OH)_2$ and nano-Cu were near the arbitrary cutoff value of 1 at all time points in all waters, indicating very broad size distributions. Average aggregate size and statistical groupings for all three ENMs can be found in Table 3. Average

Table 3. Mean Aggregate Diameter Across All Time Points (nano-CuO) or from 10−60 min ($Cu(OH)_2$ and nano-Cu)[a]

	$Cu(OH)_2$	nano-Cu	nano-CuO
aqueous matrix	mean diameter (nm)	mean diameter (nm)	mean diameter (nm)
seawater	1140[a]	1760[ab]	416[a]
lagoon water	1140[a]	1670[ab]	415[a]
50% seawater	816[a]	1990[a]	402[a]
wastewater	776[a]	994[cd]	400[a]
groundwater	884[a]	1360[c]	321[b]
hydroponic media	1040[a]	1180[c]	407[a]
storm runoff	846[a]	1600[bc]	258[c]
freshwater	958[a]	791[d]	245[c]

[a]Letters represent statistical grouping based on Tukey's test ($Cu(OH)_2$) or Kruskal−Wallis tests with multiple comparisons (nano-Cu and nano-CuO). Waters are arranged in order of decreasing ionic strength.

$Cu(OH)_2$ aggregate size in the third phase did not vary significantly with water type (ANOVA, $F_{7,803} = 0.854$, $p > 0.5$), which may be due to the large proportion (>70 wt %) of dispersants and other non-Cu ingredients in Kocide 3000. However, despite its high polydispersity, nano-Cu aggregate size correlated significantly with water type (Kruskal−Wallis, H = 149.3, 7 d.f., $p << 0.0001$). Nano-Cu aggregate size correlated well with IS except in wastewater and storm runoff, which had the highest organic contents of the waters tested by a wide margin. In wastewater, nano-Cu aggregates were smaller than would be predicted by its moderate ionic strength, but aggregates in storm runoff were comparable to those found in the most saline waters. This counterintuitive behavior may be explained by the very low rate of sedimentation of nano-Cu in storm runoff (section 3.2) resulting in larger aggregates being retained in the zone measured by DLS.

Nano-CuO displayed markedly different aggregation trends than the other two particles, aggregates being on average smaller (Figure 1) and more monodisperse with PDIs ranging from 0.24−0.36. Additionally, aggregate size significantly increased with time in all waters except freshwater and storm runoff, where aggregate size decreased (linear models, $p < 0.001$ in all cases). Given that there was very little sedimentation or dissolution in these two waters over the measurement period (see sections 3.2 and 3.3), it appears that the low IS of the storm runoff and freshwater media caused disaggregation to occur. Further evidence for this can be found in previous work,[3] which showed that nano-CuO aggregate size decreased over time in Nanopure water with up to 10 mM NaCl (equivalent to 354 mg L^{-1} Cl^-) but that at higher ionic strength aggregation occurred. Table 3 shows nano-CuO aggregation has a strong positive correlation with IS for all waters but hydroponic media. The large average aggregate size in hydroponic media is likely a result of the decrease in electrostatic repulsion between particles caused by the pH of the media being near the isoelectric point (IEP) for nano-CuO (Figure S2).

3.2. Sedimentation. Sedimentation kinetics for nano-Cu, $Cu(OH)_2$, and nano-CuO over 6 h are shown in Figure 2. In general, sedimentation follows our hypothesis and shows a positive relationship with ionic strength and an inverse relationship with organic content. However, all three particles show different trends depending on their specific composition, and nano-CuO exhibited an unpredicted stabilizing effect due to the presence of phosphate. $Cu(OH)_2$ remained relatively well suspended in all waters but groundwater likely due to the proprietary organic dispersants included in its formulation, which give it a high surface charge[3] and a low bulk density (0.617 g cm^{-3}).[2] Nano-Cu was stable in high TOC waters, namely wastewater and storm runoff, and unstable in the rest. The instability of nano-Cu in hydroponic media may have been due to the low pH of the media causing increased dissolution and subsequent formation of insoluble $Cu_3(PO_4)_2$ precipitate (Figure S8). Interestingly, aggregate size does not seem to correlate with sedimentation rate in any of the three ENMs tested here. This suggests that aggregate density (fractal aggregates vs flocs), stabilizing coatings, and dissolution/precipitation may be more important predictors of sedimentation rate.

Regardless of dispersants or oxidation state, all three particles were unstable in groundwater. This was likely due to the high bicarbonate (HCO_3^-) and low chloride concentrations found in groundwater, resulting in the formation of insoluble copper carbonates. Speciation modeling predicts that in groundwater all three particles will precipitate as malachite ($Cu_2CO_3(OH)_2$) at equilibrium (Figures S8−S10). Lagoon water and seawater also had relatively high amounts of HCO_3^-, but due to their high Cl^- content, atacamite ($Cu_2Cl(OH)_3$) is predicted to be the dominant form at equilibrium. This suggests that these particles are unstable in saline waters.

The trends in nano-CuO sedimentation rates can largely be explained as functions of water ionic strength and phosphate content, with waters being grouped into those with and without detectable PO_4^{3-} and IS accounting for order within those groups (Figure 2). For example, waters with undetectable (<0.02 mg L^{-1}) levels of PO_4^{3-} (groundwater, diluted seawater, and seawater) had the highest sedimentation rates by a wide margin and showed increasing sedimentation with increasing IS. To further investigate these trends, the ζ-potential, pH, and sedimentation rates of nano-CuO in Nanopure water with increasing PO_4 were measured. Nano-CuO sedimentation rates across a range of seawater/freshwater mixtures were also measured.

Figure 3 shows that sedimentation rate increases linearly with IS and slows over time. This has implications for estuarine environments and other areas where waters of varying salinity mix, as it suggests nano-CuO and similar ENMs may sediment from the water column when moving from areas of low salinity

DOI: 10.1021/es504918q
Environ. Sci. Technol. 2015, 49, 2749−2756

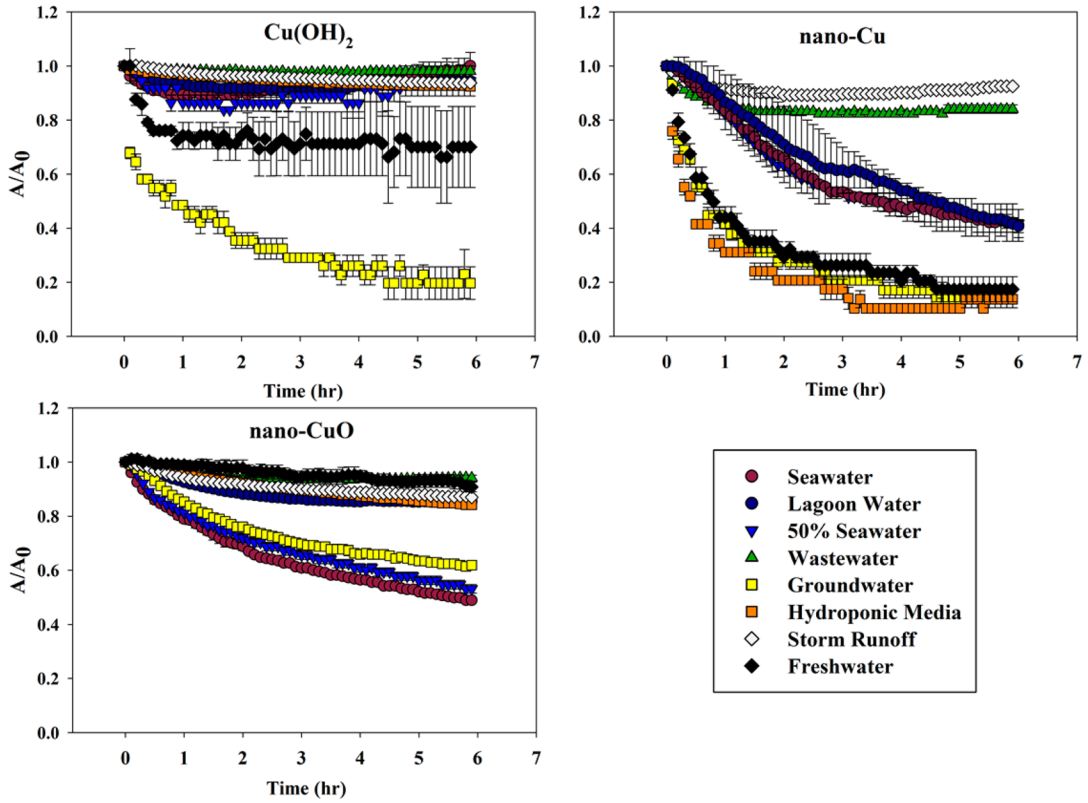

Figure 2. Sedimentation kinetics for $Cu(OH)_2$, nano-Cu, and nano-CuO. Nano-Cu in seawater, diluted seawater (50% seawater), and lagoon water was measured at a higher wavelength from a starting concentration of 20 mg L^{-1} due to the formation of interfering copper chloride compounds. Error bars represent standard error.

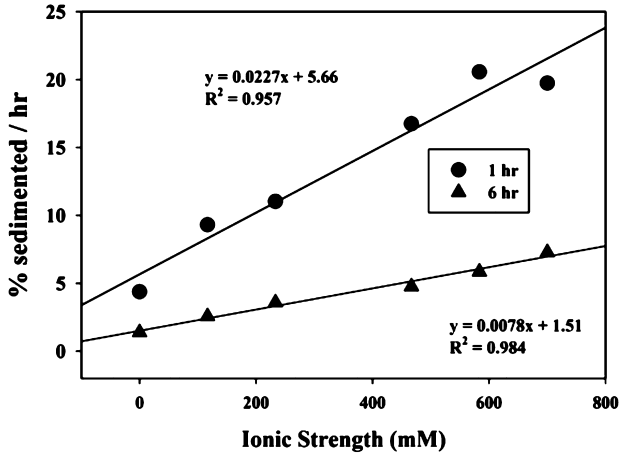

Figure 3. Nano-CuO sedimentation rates over 1 or 6 h as a function of ionic strength (in mM). Diagonal lines represent lines of best fit from linear models described.

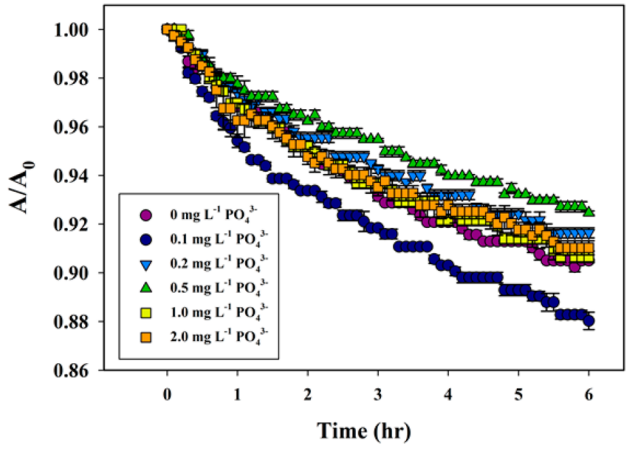

Figure 4. Sedimentation of nano-CuO in Nanopure water in the presence of increasing concentrations of PO_4^{3-} (±SE).

to areas of high salinity. Figure 4 shows that PO_4^{3-} has a variable effect on the sedimentation rate of nano-CuO in Nanopure water, causing increased sedimentation at the lowest concentration (0.1 mg L^{-1}), decreased sedimentation from 0.2 to 0.5 mg L^{-1}, and having no effect at 1.0 or 2.0 mg L^{-1} PO_4^{3-}.

Phosphate is well-known for its ability to covalently bond to metal oxides,[27,28] giving the potential to significantly alter their surface properties. Figure 5 shows that even at relatively low concentrations of PO_4^{3-} (0.1 mg L^{-1}), the ζ-potential (surface charge) of nano-CuO switches from positive to negative and becomes increasingly negative with increasing PO_4^{3-} concentrations. This change in ζ-potential is likely due to the formation of a negatively charged layer of copper phosphate on the surface of the ENMs resulting in enhanced electrostatic repulsion, leading to the effects shown in Figure 4. The nonlinear effect on sedimentation seen at higher PO_4^{3-} concentrations may be due to covalent bridging between phosphate-coated particles.

While the addition of PO_4^{3-} (as NaH_2PO_4) slightly increases the pH of the suspension (~0.1 pH units), its effect on ζ potential is greater than what is predicted for the small change in pH observed (~0.1 pH units). For example, Figure S2 predicts a ζ potential of 0 at pH 6, but the addition of 2.0 mg

DOI: 10.1021/es504918q
Environ. Sci. Technol. 2015, 49, 2749−2756

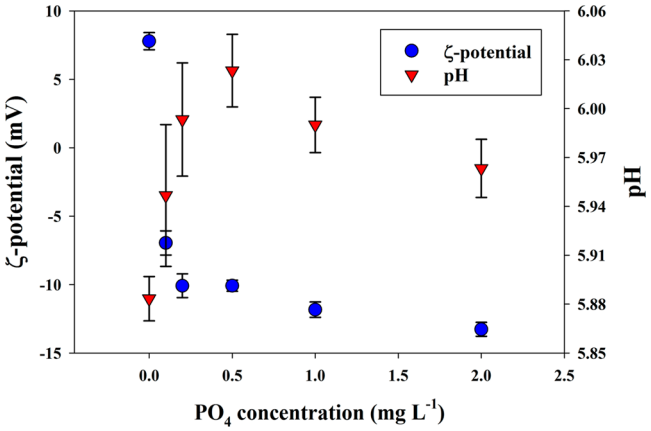

Figure 5. ζ potential and pH of nano-CuO in Nanopure water in the presence of increasing concentrations of PO_4^{3-} (±SE).

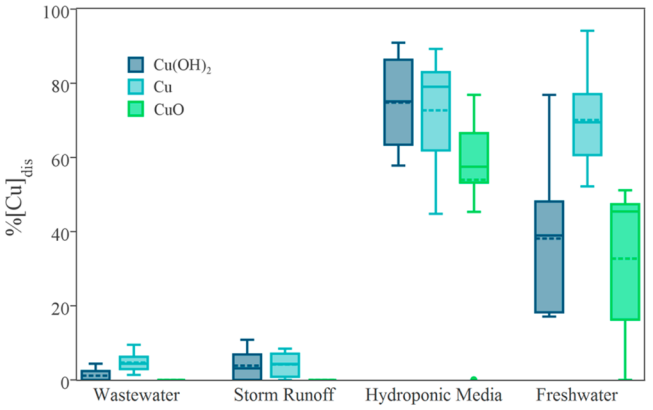

Figure 7. Tukey boxplots of ENM dissolution in four natural waters as a percentage of total aqueous phase copper (Cu_{aq}). $\%[Cu]_{dis}$ did not vary significantly over time (linear models, $p > 0.05$) except for $Cu(OH)_2$ in storm runoff ($R^2 = 0.507$, $F_{1,7} = 6.16$, $p = 0.05$) so box plots represent dissolution from all time points. Dashed lines represent means. Seawater, diluted seawater, lagoon water, and groundwater are not included here due to the presence of interfering ions.

L^{-1} PO_4^{3-} results in a decrease in the ζ potential from +7.79 to −12.2 mV at the same pH. Figure S2 also shows the relationship between pH and ζ potential for nano-Cu and $Cu(OH)_2$ and may explain why the presence of PO_4^{3-} did not have a large impact on their behavior in the waters tested. The addition of even low concentrations of PO_4^{3-} to nano-CuO suspensions resulted in the polarity of the particle surface charges switching from positive to negative, but both nano-Cu and $Cu(OH)_2$ are negatively charged throughout the whole range of pH tested. Consequently, any sorption of PO_4^{3-} on the surfaces of these particles is not likely to influence their behavior.

3.3. Dissolution. The total amount of aqueous phase copper (Cu_{aq}, Figure 6) and the fraction of ionic copper in Cu_{aq} ($\%[Cu]_{dis}$, Figure 7) for the three ENMs varied with pH and TOC, as hypothesized, but also with ionic strength. Cu_{aq} was generally stable over the course of the experiment but tended to increase after ∼60 days, indicating that some long-term dissolution may have been occurring. For $Cu(OH)_2$ and nano-CuO in hydroponic media (pH 5.87), dissolution to ionic Cu is significant even in the presence of complex-forming ions. In freshwater (pH 6.32), the presence of NOM reduces Cu_{aq} and Cu_{dis}, possibly through a combination of chelation and by coating particle surfaces. A further decrease in Cu_{dis} (to 0% for nano-CuO) is seen in storm runoff, which at 6.49 mg C L^{-1} has the highest TOC content of the waters tested (Figure 7).

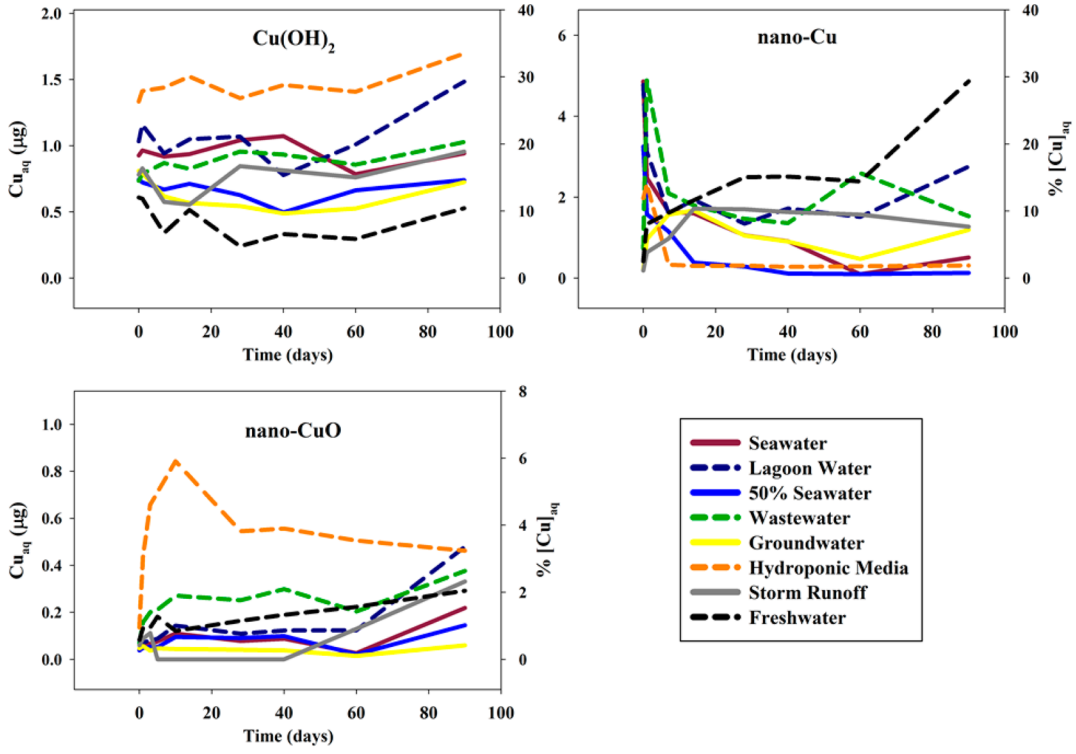

Figure 6. Aqueous phase Cu by mass (μg, left axis) and by percent of initial Cu (right axis) for $Cu(OH)_2$, nano-Cu, and nano-CuO in natural waters over 90 days. Note scale changes of *y* axes.

DOI: 10.1021/es504918q
Environ. Sci. Technol. 2015, 49, 2749−2756

Nano-Cu displayed markedly different dissolution behavior than $Cu(OH)_2$ and nano-CuO, likely due to it being the only ENM tested here present in a nonoxidized form. In all but the three least saline waters (groundwater, storm runoff, freshwater), Cu_{aq} spiked to 20−30% at day 0 or 1 before rapidly decreasing to relatively low levels. This may have been due to the precipitation of dissolved ions as complexes like $Cu_2Cl(OH)_3$, CuO, and $Cu_3(PO_4)_2$ (Figure S8). In waters with detectable organic content (e.g., wastewater and storm runoff), the complexation of ionic Cu by large ligands seems to also play a role in lowering Cu_{dis}. This can be seen in Figure 7, which shows that in wastewater (TOC = 2.38 mg L^{-1} C) less than 10% of Cu_{aq} from nano-Cu was composed of free ions. The relatively high concentration of NOM in storm runoff appears to have slowed nano-Cu dissolution while producing a similarly low proportion of Cu_{dis} to Cu_{aq} due to chelation by organic compounds.[29]

3.4. Environmental Implications. Stability, in terms of aggregation, sedimentation, and dissolution, is important in determining the fate, transport, and toxicity of ENMs in environmental media. The three particles studied here all display different behaviors and appear to be controlled by different water properties. $Cu(OH)_2$ forms large aggregates or flocs under all the conditions tested here that were relatively well suspended. Nano-Cu is also well suspended in waters with high organic contents, while the presence of phosphate appears to be the main controlling factor for nano-CuO sedimentation. For nano-CuO, the shift from positive to negative surface charge that was caused by phosphate may also influence the fate and toxicology of these and other metal oxide ENMs, by altering their interactions with ions and other charged surfaces. For example, clay particles suspended in natural waters can act as carriers for charged particles and transport ENMs much further than they would otherwise,[30] but this effect is very sensitive to changes in electrochemistry[31] and may be altered by changes in ENM surface charge.

At low pH, Cu-based ENMs will undergo some degree of dissolution, which will likely depend on the composition of both the ENM and the aqueous media. Additionally, in waters with medium to high concentrations of Cl^-, SO_4^{2-}, PO_4^{3-}, and/or HCO_3^-, copper ions will likely form insoluble or sparingly soluble inorganic complexes that may sediment from the water column. Previous research[29] has shown that Cu ions will become chelated or bound in organic complexes in waters with high organic content, although both the concentration and the specific composition of the organic compounds play a role in determining ENM behavior.[3] Since Cu ions are well-known to be toxic to many organisms,[32−34] processes that lower the amount of free Cu ions in solution may reduce the overall hazard of these ENMs. However, Cu ENM toxicity has been attributed to both ionic[22,35] and nanospecific[19,21,23,24] toxic effects, so even in waters with high organic content Cu-based ENMs may still pose a threat to aquatic organisms.

The results presented here outline the complexity in predicting the fate of copper ENMs through environmentally relevant media. However, these data point to the importance of several key factors in the short- and long-term behavior of these particles. These include well-known water properties like ionic strength, pH, and organic content but also the presence of specific ions such as phosphate and the oxidation state of the ENM.

■ ASSOCIATED CONTENT

Supporting Information

Details on nanomaterial characterization, media collection and preparation, additional information on speciation modeling, and 11 additional figures. This material is available free of charge via the Internet at http://pubs.acs.org.

■ AUTHOR INFORMATION

Corresponding Author

*E-mail: keller@bren.ucsb.edu.

Author Contributions

The manuscript was written through contributions of all authors. All authors have given approval to the final version of the manuscript.

Notes

The authors declare no competing financial interest.

■ ACKNOWLEDGMENTS

This work was supported in part by the National Science Foundation and the U.S. Environmental Protection Agency under Cooperative Agreement # NSF-EF0830117, and by National Science Foundation Grant EF-0742521. Any opinions, findings, and conclusions or recommendation expressed in this material are those of the authors and do not necessarily reflect the views of the National Science Foundation or the U.S. Environmental Protection Agency. The authors would like to thank Arielle and Nicole Beaulieu for their assistance in carrying out these experiments, and Amanda Strom at the UCSB MRL for her help with the ICP-AES. The MRL Shared Experimental Facilities are supported by the MRSEC Program of the NSF under Award No. DMR 1121053; a member of the NSF-funded Materials Research Facilities Network.

■ ABBREVIATIONS

DLS, dynamic light scattering; ENM, engineered nanomaterials; ICP-AES, inductively coupled plasma atomic emission spectrometer; IS, ionic strength; NOM, natural organic matter; PDI, polydispersity index; TOC, total organic carbon

■ REFERENCES

(1) Keller, A. A.; McFerran, S.; Lazareva, A.; Suh, S. Global life cycle releases of engineered nanomaterials. *J. Nanopart. Res.* **2013**, *15*, No. 1692.

(2) DuPont Material Safety Data Sheet: DuPont Kocide 3000 Fungicide/Bactericide. http://www.cdms.net/LDat/mp7HK000.pdf (January 16, 2014).

(3) Adeleye, A. S.; Conway, J. R.; Perez, T.; Rutten, P.; Keller, A. A. Influence of extracellular polymeric substances on the long-term fate, dissolution and speciation of copper-based nanoparticles. *Environ. Sci. Technol.* **2014**, *48*, 12561−12568.

(4) Aazam, E. S.; Mohamed, R. M. Environmental remediation of Direct Blue dye solutions by photocatalytic oxidation with cuprous oxide. *J. Alloys Compd.* **2013**, *577*, 550−555.

(5) Akhavan, O.; Ghaderi, E. Cu and CuO nanoparticles immobilized by silica thin films as antibacterial materials and photocatalysts. *Surf. Coat. Technol.* **2010**, *205* (1), 219−223.

(6) Wang, Y. Q.; Liu, L.; Cai, Y. R.; Chen, J. J.; Yao, J. M. Preparation and photocatalytic activity of cuprous oxide/carbon nanofibres composite films. *Appl. Surf. Sci.* **2013**, *270*, 245−251.

(7) Metzler, D. M.; Li, M. H.; Erdem, A.; Huang, C. P. Responses of algae to photocatalytic nano-TiO2 particles with an emphasis on the effect of particle size. *Chem. Eng. J.* **2011**, *170* (2−3), 538−546.

(8) Zhang, S. J.; Jiang, Y. L.; Chen, C. S.; Spurgin, J.; Schwehr, K. A.; Quigg, A.; Chin, W. C.; Santschi, P. H. Aggregation, Dissolution, and

DOI: 10.1021/es504918q
Environ. Sci. Technol. 2015, 49, 2749−2756

Stability of Quantum Dots in Marine Environments: Importance of Extracellular Polymeric Substances. *Environ. Sci. Technol.* **2012**, *46* (16), 8764−8772.
(9) Miao, A. J.; Zhang, X. Y.; Luo, Z. P.; Chen, C. S.; Chin, W. C.; Santschi, P. H.; Quigg, A. Zinc oxide engineered nanoparticles dissolution and toxicity to marine phytoplankton. *Environ. Toxicol. Chem.* **2010**, *29* (12), 2814−2822.
(10) Bennett, S. W.; Adeleye, A.; Ji, Z. X.; Keller, A. A. Stability, metal leaching, photoactivity and toxicity in freshwater systems of commercial single wall carbon nanotubes. *Water Res.* **2013**, *47* (12), 4074−4085.
(11) Miller, R. J.; Bennett, S.; Keller, A. A.; Pease, S.; Lenihan, H. S. TiO_2 nanoparticles are phototoxic to marine phytoplankton. *PLoS One* **2012**, *7* (1), e30321.
(12) Israelachvili, J. N. *Intermolecular and Surface Forces*; 3rd ed.; Elsevier: 2011.
(13) Adeleye, A. S.; Keller, A. A.; Miller, R. J.; Lenihan, H. S. Persistence of commercial nanoscaled zero-valent iron (nZVI) and by-products. *J. Nanopart. Res.* **2013**, *15*, No. 1418.
(14) Yang, K.; Lin, D. H.; Xing, B. S. Interactions of Humic Acid with Nanosized Inorganic Oxides. *Langmuir* **2009**, *25* (6), 3571−3576.
(15) Adeleye, A. S.; Keller, A. A. Long-term colloidal stability and metal leaching of single wall carbon nanotubes: Effect of temperature and extracellular polymeric substances. *Water Res.* **2014**, *49*, 236−250.
(16) Van Hoecke, K.; De Schamphelaere, K. A. C.; Van der Meeren, P.; Smagghe, G.; Janssen, C. R. Aggregation and ecotoxicity of CeO2 nanoparticles in synthetic and natural waters with variable pH, organic matter concentration and ionic strength. *Environ. Pollut.* **2011**, *159* (4), 970−976.
(17) Zhao, L. J.; Hernandez-Viezcas, J. A.; Peralta-Videa, J. R.; Bandyopadhyay, S.; Peng, B.; Munoz, B.; Keller, A. A.; Gardea-Torresdey, J. L. ZnO nanoparticle fate in soil and zinc bioaccumulation in corn plants (Zea mays) influenced by alginate. *Environ. Sci.: Processes Impacts* **2013**, *15* (1), 260−266.
(18) Shah, V.; Dobiasova, P.; Baldrian, P.; Nerud, F.; Kumar, A.; Seal, S. Influence of iron and copper nanoparticle powder on the production of lignocellulose degrading enzymes in the fungus Trametes versicolor. *J. Hazard. Mater.* **2010**, *178* (1−3), 1141−1145.
(19) Shi, J.; Abid, A. D.; Kennedy, I. M.; Hristova, K. R.; Silk, W. K. To duckweeds (Landoltia punctata), nanoparticulate copper oxide is more inhibitory than the soluble copper in the bulk solution. *Environ. Pollut.* **2011**, *159* (5), 1277−1282.
(20) Wang, Z. Y.; Xie, X. Y.; Zhao, J.; Liu, X. Y.; Feng, W. Q.; White, J. C.; Xing, B. S. Xylem- and Phloem-Based Transport of CuO Nanoparticles in Maize (Zea mays L.). *Environ. Sci. Technol.* **2012**, *46* (8), 4434−4441.
(21) Hanna, S. K.; Miller, R. J.; Zhou, D. X.; Keller, A. A.; Lenihan, H. S. Accumulation and toxicity of metal oxide nanoparticles in a soft-sediment estuarine amphipod. *Aquat. Toxicol.* **2013**, *142*, 441−446.
(22) Blinova, I.; Ivask, A.; Heinlaan, M.; Mortimer, M.; Kahru, A. Ecotoxicity of nanoparticles of CuO and ZnO in natural water. *Environ. Pollut.* **2010**, *158* (1), 41−47.
(23) Buffet, P. E.; Richard, M.; Caupos, F.; Vergnoux, A.; Perrein-Ettajani, H.; Luna-Acosta, A.; Akcha, F.; Amiard, J. C.; Amiard-Triquet, C.; Guibbolini, M.; Risso-De Faverney, C.; Thomas-Guyon, H.; Reip, P.; Dybowska, A.; Berhanu, D.; Valsami-Jones, E.; Mouneyrac, C. A Mesocosm Study of Fate and Effects of CuO Nanoparticles on Endobenthic Species (Scrobicularia plana, Hediste diversicolor). *Environ. Sci. Technol.* **2013**, *47* (3), 1620−1628.
(24) Gomes, T.; Pinheiro, J. P.; Cancio, I.; Pereira, C. G.; Cardoso, C.; Bebianno, M. J. Effects of copper nanoparticles exposure in the mussel *Mytilus galloprovincialis*. *Environ. Sci. Technol.* **2011**, *45* (21), 9356−9362.
(25) Wang, Z.; von dem Bussche, A.; Kabadi, P. K.; Kane, A. B.; Hurt, R. H. Biological and Environmental Transformations of Copper-Based Nanomaterials. *ACS Nano* **2013**, *7* (10), 8715−8727.
(26) Lee, J. D. *Concise Inorganic Chemistry/J.D. Lee*; Chapman & Hall: London, 1991.
(27) Boehm, H. P. Acidic and basic properties of hydroxylated metal oxide surfaces. *Discuss. Faraday Soc.* **1971**, *52* (0), 264−275.
(28) Daou, T. J.; Begin-Colin, S.; Grenèche, J. M.; Thomas, F.; Derory, A.; Bernhardt, P.; Legaré, P.; Pourroy, G. Phosphate Adsorption Properties of Magnetite-Based Nanoparticles. *Chem. Mater.* **2007**, *19* (18), 4494−4505.
(29) Sunda, W. G.; Hanson, A. K. Measurement of free cupric ion concentration in seawater by a ligand competition technique involving copper sorption onto C-18 SEP-PAK cartriges. *Limnol. Oceanogr.* **1987**, *32* (3), 537−551.
(30) Abdel-Fattah, A. I.; Zhou, D. X.; Boukhalfa, H.; Tarimala, S.; Ware, S. D.; Keller, A. A. Dispersion Stability and Electrokinetic Properties of Intrinsic Plutonium Colloids: Implications for Subsurface Transport. *Environ. Sci. Technol.* **2013**, *47* (11), 5626−5634.
(31) Zhou, D. X.; Abdel-Fattah, A. I.; Keller, A. A. Clay Particles Destabilize Engineered Nanoparticles in Aqueous Environments. *Environ. Sci. Technol.* **2012**, *46* (14), 7520−7526.
(32) Moore, M. N.; Widdows, J.; Cleary, J. J.; Pipe, R. K.; Salkeld, P. N.; Donkin, P.; Farrar, S. V.; Evans, S. V.; Thomson, P. E. Responses of the Mussel *Mytilus edulis* to Copper and Phenanthrene - Interactive Effects. *Mar. Environ. Res.* **1984**, *14* (1−4), 167−183.
(33) Sunda, W. G.; Guillard, R. R. L. Relationship between cupric ion activity and toxicity of copper to phytoplankton. *J. Mar. Res.* **1976**, *34* (4), 511−529.
(34) Flemming, C. A.; Trevors, J. T. Copper Toxicity and Chemistry in the Environment - a Review. *Water Air Soil Pollut.* **1989**, *44* (1−2), 143−158.
(35) Franklin, N. M.; Rogers, N. J.; Apte, S. C.; Batley, G. E.; Gadd, G. E.; Casey, P. S. Comparative toxicity of nanoparticulate ZnO, bulk ZnO, and ZnCl2 to a freshwater microalga (Pseudokirchneriella subcapitata): The importance of particle solubility. *Environ. Sci. Technol.* **2007**, *41* (24), 8484−8490.

DOI: 10.1021/es504918q
Environ. Sci. Technol. 2015, 49, 2749−2756